

# Neutron Collimation With Microchannel Plates: Calibration of Existing Technology and Near Future Possibilities

Anton S. Tremsin, Daniel S. Hussey, R. Gregory Downing, W. Bruce Feller, David F. R. Mildner,  
David L. Jacobson, Muhammad Arif, and Oswald H. W. Siegmund

**Abstract**—A new type of high performance and compact neutron collimator can be manufactured from Gd- or B-doped microchannel plates (MCPs). Structures only a few mm thick have very narrow rocking curves and high out-of-angle rejection ratios, as observed previously with a cold neutron beam. We present the results of measurements with a collimated ( $L/D$  ratio  $\sim 280 : 1$ ) thermal neutron beam. MCP collimators doped with 3 mole % of  $^{nat}\text{Gd}_2\text{O}_3$  as well as doped with 10 mole % of  $^{10}\text{B}_2\text{O}_3$  were calibrated for transmission versus tilt angle. The MCPs used in this study were only 0.6 and 0.8 mm thick with  $\sim 8.5 \mu\text{m}$  circular pores on 11.5  $\mu\text{m}$  centers. All the measured rocking curves agree well with the theoretically predicted performance. Both experimental and modeling results indicate that very efficient MCP collimators (with  $< 0.1^\circ$  wide rocking curves and a rejection ratio exceeding  $10^3$ ) can be built with the existing technology.

The possibility to manufacture collimators with very large  $L/D$  ratios exceeding 1000:1 is also discussed for the case of unetched MCPs. The peak transmission of such devices with very sharp rocking curves will be limited to  $\sim 40\%$  by the transmission of the undoped glass. Application of MCP collimators for scatter rejection in neutron radiography is also considered in terms of possible image distortions, which are shown to occur only for the systems with detector spatial resolution better than 20  $\mu\text{m}$  FWHM.

**Index Terms**—Collimators, neutron optics, neutron scattering.

## I. INTRODUCTION

**I**N most neutron scattering experiments the angular spread of the neutron beam is defined by the quality of the neutron collimator. Soller slit collimators, comprising an array of absorbing films (e.g., Gd layer) separated by neutron-transparent spacers (e.g., Si wafers) [1], [2] as well as honeycomb-like packed structures [3] are widely used to shape the neutron beam. In order to achieve a high degree of collimation the thickness of the spacers should be optimized relative to the length of the structure and the

thickness of absorbing coatings. In other words the  $L/D$  aspect ratio of the collimating structure (the ratio of its length to the thickness of transmitting channel) has to be large for efficient collimators.

Compact collimators currently produced use stacked arrays of thin single-crystal silicon wafers ( $\sim 160 \mu\text{m}$  thick) with absorbing Gd coatings. Our theoretical predictions supported by preliminary experiments with cold neutrons indicate that MCP collimators can have substantially better efficiencies than existing structures [4], [5]. Current MCP technology allows for manufacturing of the structures with length to diameter ratios of up to 250:1 with active areas up to  $10 \times 10 \text{ cm}^2$ . The diameter of MCP pores can be  $< 10 \mu\text{m}$ , making these collimators very compact. Moreover, the geometry of the pores can be controlled in order to achieve the optimal collimation in the two directions separately. In addition to beam shaping, these compact structures can be used for the rejection of scattered neutrons, which degrade the quality of images in high resolution neutron radiography.

Recently, modification of MCP base glass materials through incorporation of high neutron cross-section elements such as boron and gadolinium, has resulted in MCPs capable of direct imaging detection [6]–[9] as well as collimation of neutrons [4], [5]. The glass mixture in these novel MCPs contains neutron absorbing gadolinium or boron atoms, while the rest of the manufacturing procedures remain the same. Neutron sensing microchannel plates are currently being produced for high-resolution neutron counting (with spatial resolution as small as  $\sim 20 \mu\text{m}$  and temporal resolution of  $\sim 1 \mu\text{s}$ ). Our theoretical studies indicate that these detectors should indeed have very high detection efficiency for thermal and cold neutrons [10] and achieve high spatial resolution. The spatial resolution of such detectors for UV and X-ray photons has already reached the 10  $\mu\text{m}$  level [11], and we believe the progress in MCP photon detection can be extended to neutron imaging with spatial resolution of  $\sim 20 \mu\text{m}$  and below.

Our first experimental measurements of Gd-doped MCP collimation performed with a cold neutron beam, proved the efficiency of these compact structures [4]. The results of these measurements also support the validity of our theoretical efficiency calculations, which can be used to predict the ultimate performance of MCP collimators using existing manufacturing technology. In this paper we extend our experimental studies of MCP collimators to a thermal neutron beam and compare the results of these measurements with predicted performance. We

Manuscript received June 1, 2006; revised December 18, 2006.

A. S. Tremsin and O. H. W. Siegmund are with the Space Sciences Laboratory, University of California, Berkeley, Berkeley, CA 94720 USA (e-mail: ast@ssl.berkeley.edu; ossy@ssl.berkeley.edu).

D. S. Hussey, R. G. Downing, D. F. R. Mildner, D. L. Jacobson, and M. Arif are with the National Institute of Standards and Technology, Gaithersburg, MD 20899 USA (e-mail: daniel.hussey@nist.gov; gregory.downing@nist.gov; david.mildner@nist.gov; david.jacobson@nist.gov; muhammad.arif@nist.gov).

W. B. Feller is with NOVA Scientific Inc., Sturbridge, MA 01566 USA (e-mail: bfeller@novascientific.com).

Color versions of one or more of the figures in this paper are available online at <http://ieeexplore.ieee.org>.

Digital Object Identifier 10.1109/TNS.2007.891080

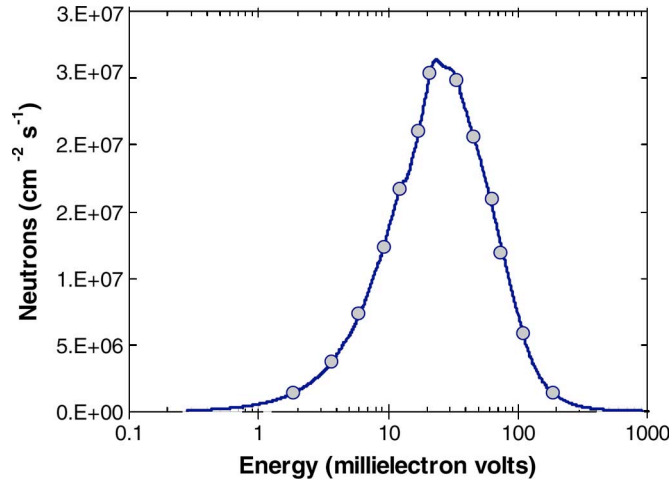


Fig. 1. The neutron spectrum of the beam used in MCP collimation measurements [12]. The beam has an aspect ratio of 280:1.

also discuss the possibility for manufacturing unetched MCP collimators with very large  $L/D$  ratios and therefore very sharp rocking curves. Finally, the application of MCP collimators for scatter rejection in neutron radiography is discussed in terms of possible image degradation, shown to occur only if the detector spatial resolution is better than  $20 \mu\text{m}$ .

## II. THERMAL NEUTRON COLLIMATION

### A. Hollow Pore (Etched) MCP Collimators

The etched microchannel plates used in the present experimental study with thermal neutrons were not optimized for collimation applications but rather were constructed for neutron detection. We have investigated the performance of a 0.6 mm thick (aspect ratio or  $L/D = 69 : 1$  for MCP1) and a 0.8 mm thick ( $L/D = 94 : 1$  for MCP2) MCPs with  $8.5 \mu\text{m}$  circular pores packed hexagonally with center-to-center spacing of  $11.5 \mu\text{m}$ . The glass in these structures was doped with a combination of 3 mole % of  $^{nat}\text{Gd}_2\text{O}_3$  plus 2 mol% of  $^{10}\text{B}_2\text{O}_3$  for MCP1, and 10 mole % of  $^{10}\text{B}_2\text{O}_3$  alone for MCP2. The MCPs were 33 mm in diameter and thus contained several million microchannels with an open area ratio of  $\sim 50\%$ .

The measurements of collimator transmission as a function of tilt angle were carried out at the neutron imaging facility at NIST Center for Neutron Research, Gaithersburg, MD, USA. The neutron beam has an  $L/D$  ratio of  $\sim 280 : 1$  and its spectrum is shown in Fig. 1. The rocking curves were measured with an amorphous silicon detector in direct contact with a ZnS scintillator doped with  $^6\text{LiF}$ . The transmission was measured by dividing the image of the collimator by a flat field, and averaging over a region inside the MCP collimator. The uncertainty of the transmission measurements was the standard deviation of the transmission of the region and found to be better than 1.5%. A detailed description of the beamline can be found in [12].

Fig. 2 shows the MCP transmission as a function of the beam incidence angle relative to the MCP normal (rocking curves) measured for MCP1 and MCP2. The width of the rocking curve for Gd/B-doped MCP [Fig. 2(a)] was found to be  $\pm 1^\circ$ . The peak transmission was 56 % and out-of-angle rejection ratio was

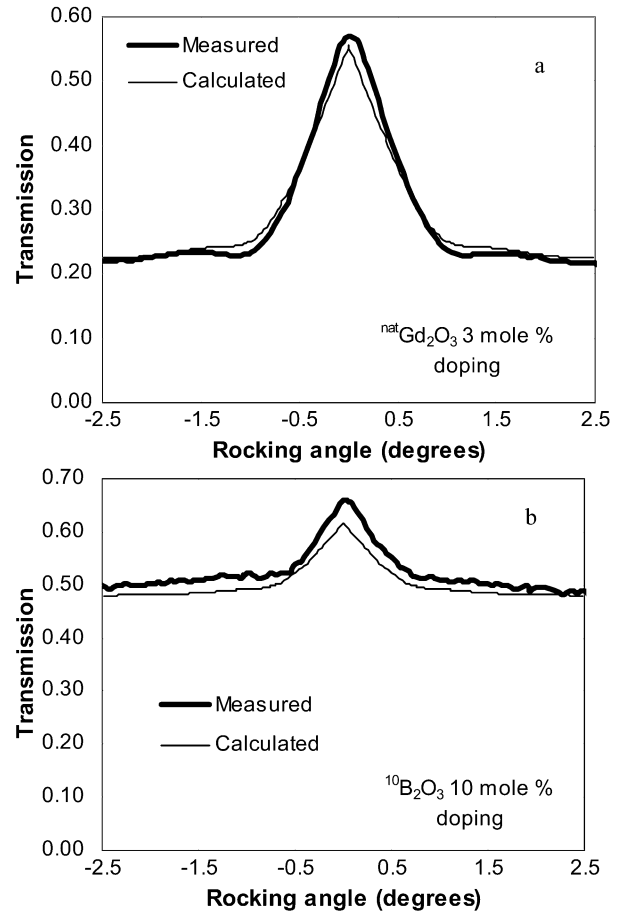


Fig. 2. The measured (bold line) and predicted (fine line) rocking curves of etched (hollow pore) microchannel plates. (a) The 0.6 mm thick MCP is doped with 3 mole % of  $^{nat}\text{Gd}_2\text{O}_3$  plus 2 mol%  $^{10}\text{B}_2\text{O}_3$ . (b) The 0.8 mm thick MCP is doped with 10 mole % of  $^{10}\text{B}_2\text{O}_3$ . MCP pores are  $8.5 \mu\text{m}$  in diameter with center-to-center spacing  $11.5 \mu\text{m}$ . A thermal neutron beam with a spectrum shown in Fig. 1 having an average energy of  $\sim 25$  meV and beam  $L/D$  ratio of 280:1 is used in the measurements. Calculated curve corresponds to monoenergetic transmissions (at energies shown by circles in Fig. 1) convolved into transmission for the beam with spectrum shown in Fig. 1.

2.5:1. The B-doped MCP [Fig. 2(b)] showed 66% peak transmission and 1.3 rejection ratio for angles  $< 0.75^\circ$  off normal incidence. We want to emphasize that these characteristics are far from optimal and can be substantially improved for collimation-optimized MCP structures producible with the existing technology. Much thicker ( $L/D$  up to 250:1) and therefore more efficient MCP collimators with etched pores can be produced. In addition, microchannel plate neutron collimators can have  $L/D$  ratios as high as several thousand if the core glass is left unetched (Section II.B).

We have used our model of neutron absorption within MCP glass [4]–[6] to predict the collimation efficiency for the MCPs tested in the present study. The transmission of an MCP with a given geometry and doping concentrations is calculated from the following equation:

$$T_{\text{MCP}} = 1 - P_{\text{absorb}}(\alpha) \\ = 1 - \exp\left(-L_{\text{eff}}(\alpha) \sum N_i \sigma_i\right)$$

where  $N_i$  is the number of neutron-absorbing atoms of a particular material  $i$  per unit volume of the MCP glass,  $\sigma_i$  is the

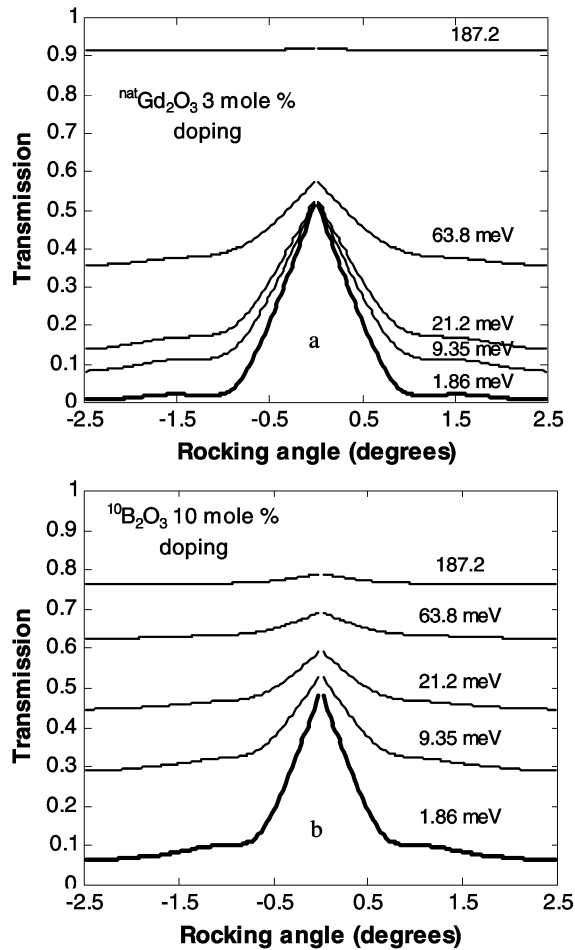


Fig. 3. The predicted rocking curves of an etched (hollow pore) microchannel plate collimator calculated for neutron beams of different energies. All MCP parameters are the same as in Fig. 2. The notation for the neutron energy in the graph is in millielectron volts.

cross section for the neutron capture reaction by those atoms, and  $L_{\text{eff}}$  is the length of neutron trajectory contained within the MCP glass for the neutrons incident at angle  $\alpha$  relative to MCP normal. A detailed description of the way the parameters  $N_i$  and  $L_{\text{eff}}$  are calculated can be found in the [4]–[6].

The predicted transmission for monoenergetic neutron beams of different energies calculated for MCP1 and MCP2 are shown in Fig. 3. Obviously the transmission strongly depends on the neutron energy as the thermal neutron absorption cross section varies inversely with the square root of the neutron energy [13]. These calculations indicate that the collimation of MCP1 is already quite efficient for cold neutrons, despite its very small thickness of only 0.6 mm. The dashed lines in Fig. 2 correspond to the rocking curves obtained by an integration of monoenergetic curves in accordance with the beam spectrum shown in Fig. 1. The good agreement between the predicted and measured transmission curves prove the accuracy of our collimator theory, which can be successfully used to optimize the performance of future collimation-dedicated MCPs. Thus we can optimize the maximum peak transmission, out-of-angle rejection ratio and acceptance angles independently for both directions of collimation. Our model predicts that for a beam with a spectrum similar to the one shown in Fig. 1 the rocking curves of etched

TABLE I  
THERMAL NEUTRON SCATTERING ( $\sigma_s$ ) AND ABSORPTION ( $\sigma_a$ ) CROSS SECTIONS [13] OF ELEMENTS IN STANDARD MCP GLASS (TO BE USED IN UNETCHED COLLIMATORS) AND RESULTING NEUTRON ATTENUATION FOR DIFFERENT MCP THICKNESSES. PORES ARE 10  $\mu\text{m}$  IN DIAMETER, WALLS 2  $\mu\text{m}$

Element	$\sigma_s$ barns	$\sigma_a$ barns	attenuation for L/D=	
			500:1	1000:1
Si	2.167	0.171	0.0175	0.0348
Pb	11.12	0.171	0.0299	0.0589
K	1.96	2.1	0.0051	0.0102
Rb	6.8	0.38	0.0018	0.0036
O	4.232	0.0002	0.0765	0.1471
Glass attenuation			0.1271	0.238
MCP peak transmission			0.550	0.480

MCP collimators built with the present technology ( $^{nat}\text{Gd}_2\text{O}_3$  doped 250:1 L/D MCPs) can be as narrow as  $\sim 10$  mrad with peak transmission above 60%.

### B. Unetched Collimators With Large L/D Ratios

Standard electron multiplying MCPs require a manufacturing step where the pores in the solid-glass structure are acid-etched to form microchannels. As mentioned earlier, the length-to-diameter ratio of the etched MCP is limited by the core glass etching process. The pre-etching glass disk consists of an array of core glass cylinders (6–15  $\mu\text{m}$  in dimension) surrounded by cladding glass of a slightly different composition. The glass mixture of the core glass is etchable by proper choice of acid, while the cladding glass is not dissolved by that solvent. The etch depth into the wafer or disk limits current MCPs to L/D ratios of  $\sim 250:1$ . However, MCP collimators can have unetched core glass and thus be produced with L/D ratios exceeding several thousand with correspondingly very sharp rocking curves. The transmission of unetched core glass must obviously be quite high in order to produce collimators with reasonable peak transmission.

We have performed detailed analysis of the MCP glass transmission similar to the analysis of [6]. The calculated neutron attenuation due to absorption and scattering for each glass constituent and the calculated resulting peak transmission of a typical unetched MCP geometry of 10  $\mu\text{m}$  pores, are shown in Table I. Fig. 4 shows the glass transmission and the peak transmission of the same MCP as function of its thickness (i.e., L/D ratio). Our analysis indicates that we should be able to produce very efficient unetched MCP collimators with L/D ratios exceeding 1000:1. Estimates of their efficiency show that these thermal neutron collimators can have rocking curves as narrow as  $< 0.1^\circ$  and out-of-angle rejection ratios exceeding  $10^3$ .

### III. SCATTER REJECTION IN NEUTRON RADIOGRAPHY

Rejection of scattered neutrons in high-resolution neutron radiography may substantially improve the quality of detected images. A neutron collimator installed between the object and the detector should eliminate those neutrons that degrade the contrast and resolution of the resulting image after being scattered inside the imaged object. The transmission of the collimator has to be uniform enough so that the image is not perturbed

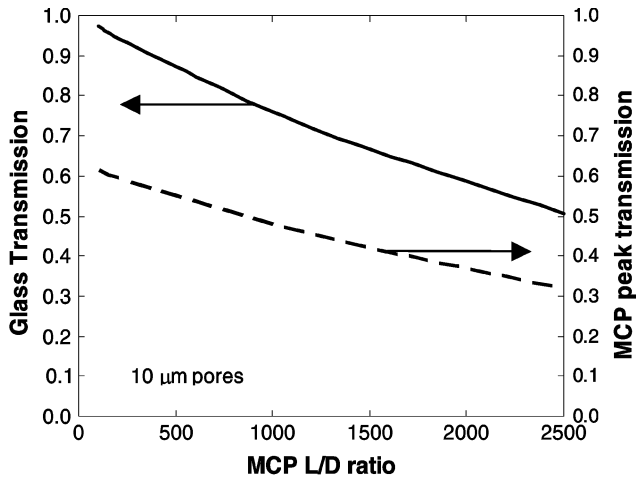


Fig. 4. The glass transmission (solid line) and MCP peak transmission (dashed line) calculated as functions of MCP L/D ratios (unetched MCP—pores are not etched and contain the core glass). The core glass does not contain atoms with high neutron absorption cross sections. The contribution of individual glass constituents is shown in Table I. The MCP transmission is calculated for an MCP with 10  $\mu\text{m}$  circular pores hexagonally packed on 12  $\mu\text{m}$  grid.

by the collimator itself. The conventional neutron collimators described in [1]–[3] have substantial variation of their transmission across the field of view. The resulting images obtained with these collimators will contain dark strips. There will also be no scatter rejection in one dimension. The transmission of MCP collimators is more uniform across the field of view as they have transparent/opaque areas varying on the scale of only  $\sim 10 \mu\text{m}$  and they also reject scattered neutrons in both dimensions simultaneously. The resulting image may have a dot-like structure with dots being on the scale of only 10  $\mu\text{m}$ , thus not quite visible with the present imaging detection technology.

We have calculated the microstructure of the transmission of a typical MCP collimator. Fig. 5 shows the resulting full-field illumination images obtained on a detector with a given spatial resolution. An image obtained with an ideal detector will have shaded areas corresponding to the MCP glass walls with almost no neutron transmission, Fig. 5(a). These areas will be smoothed to within only a few percent transmission variation with detector resolution of 10  $\mu\text{m}$  FWHM, Fig. 5(c). As seen from the Fig. 5(d), the MCP collimators used for scatter rejection do not introduce any measurable image distortions if the detector spatial resolution is not better than 20  $\mu\text{m}$  FWHM.

#### IV. CONCLUSION

The results of our experimental studies correlated with theoretical predictions indicate that very efficient MCP thermal and cold neutron collimators can be built with existing technology. Only a very limited number of MCP collimator samples of different geometry and doping concentrations were available for the experimental evaluation at a neutron beam and those MCPs were not optimal for the collimation. However, the very good agreement between the experimental and predicted performance proves the accuracy of our modeling, which predicts that collimators with very narrow rocking curves ( $< 0.1$  degree [4], [5]) can be built in the near future and allows optimization

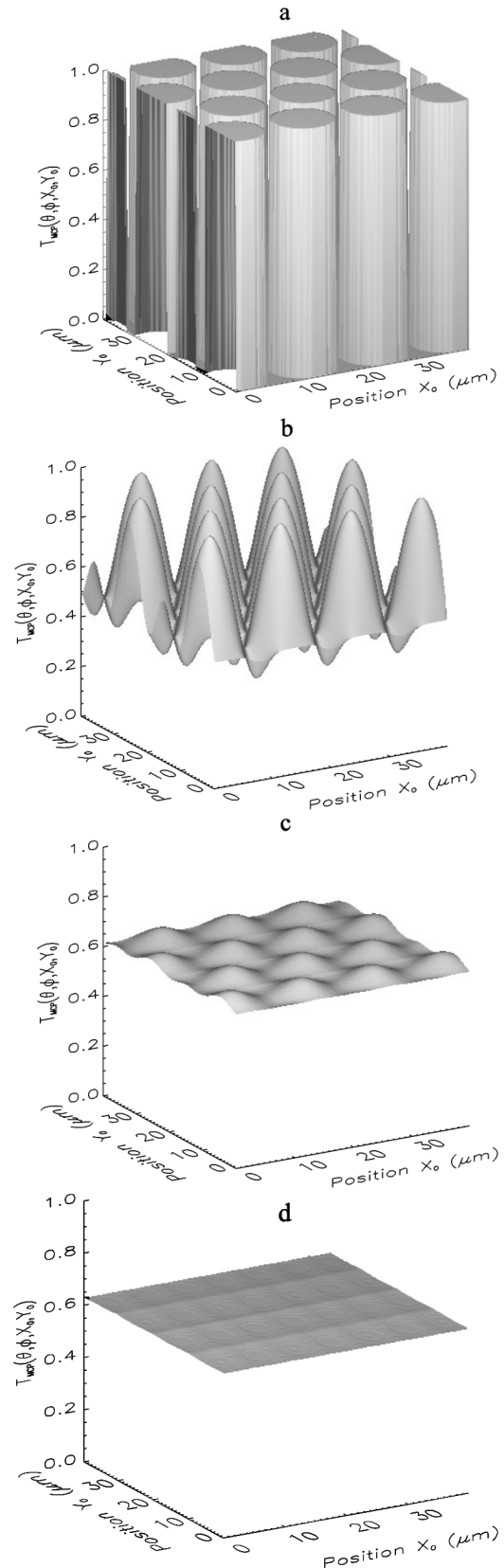


Fig. 5. The predicted full-field illumination image obtained by a detector with a given spatial resolution. The detector spatial resolution (all FWHM) is (a) infinite (ideal detector); (b) 5  $\mu\text{m}$ ; (c) 10  $\mu\text{m}$ ; (d) 20  $\mu\text{m}$ . An MCP collimator is placed in front of the detector for the rejection of scattered neutrons. The MCP has 10  $\mu\text{m}$  circular pores and 2  $\mu\text{m}$  walls, is 0.6 mm thick and is doped with 3 mole % of  $^{nat}\text{Gd}_2\text{O}_3$  and 2 mol%  $^{10}\text{B}_2\text{O}_3$ . The averaged MCP transmission is  $\sim 63\%$ .

of MCP collimators for a particular application. In particular the compromise between the highest transmission and highest out-of-angle neutron rejection can be determined in order to meet the requirements of experiments where MCP collimators can shape the neutron beam itself and/or can be used for the scatter rejection improving the quality of experimental data. Insertion of MCP collimators in the path of neutrons does not introduce any image distortions unless the detector resolution is better than  $20\ \mu\text{m}$  FWHM.

#### ACKNOWLEDGMENT

The authors would like to acknowledge the support of Neutron Imaging Facility at NIST Center for Neutron Research. A.S. Tremsin is grateful to NOVA Scientific Inc. for the assistance with neutron sensitive MCP devices.

#### REFERENCES

- [1] T. Krist, "Solid state and conventional neutron optical elements," *Nucl. Instrum. Methods Phys. Res. A*, vol. A529, pp. 50–53, 2004.
- [2] L. D. Cussen, C. J. Vale, I. S. Anderson, and P. Høghøj, "Tests of a silicon wafer based neutron collimator," *Nucl. Instrum. Methods Phys. Res. A*, vol. A471, pp. 392–397, 2001.
- [3] C. Petrillo, E. Guarini, F. Formisano, F. Sacchetti, E. Babucci, and C. Campeggi, "A honeycomb collimator for the neutron Brillouin scattering spectrometer BRISP," *Nucl. Instrum. Methods Phys. Res. A*, vol. A489, pp. 304–312, 2002.
- [4] A. S. Tremsin, W. B. Feller, and R. G. Downing, "Very compact high performance microchannel plate thermal neutron collimators," *IEEE Trans. Nucl. Sci.*, vol. 51, no. 3, pp. 1020–1024, Jun. 2004.
- [5] A. S. Tremsin and W. B. Feller, "The theory of compact and efficient circular-pore MCP neutron collimators," *Nucl. Instrum. Methods Phys. Res. A*, vol. A556, pp. 556–564, 2006.
- [6] G. W. Fraser and J. F. Pearson, "The direct detection of thermal-neutrons by imaging microchannel-plate detectors," *Nucl. Instrum. Methods Phys. Res. A*, vol. A293, pp. 569–574, 1990.
- [7] G. W. Fraser, J. F. Pearson, O. S. Al-Horayess, W. B. Feller, and L. M. Cook, "Thermal neutron imaging using microchannel plates," in *Proc. SPIE*, 1992, vol. 1737, pp. 298–307.
- [8] G. W. Fraser, G. Vourvopoulos and T. Paradellis, Eds., "Thermal neutron imaging," in *Proc. SPIE*, 1995, vol. 2339, pp. 287–301, Int. Conf. on Neutrons and Their Applications.
- [9] W. B. Feller, R. G. Downing, and P. L. White, "Neutron field imaging with microchannel plates," in *Proc. SPIE*, 2000, vol. 4141, pp. 291–302, Hard X-Ray, Gamma-Ray, and Neutron Detector Physics II.
- [10] A. S. Tremsin, W. B. Feller, and R. G. Downing, "Efficiency optimization of microchannel plate (MCP) neutron imaging detectors. I Square channels with  $^{10}\text{B}$  doping," *Nucl. Instrum. Methods Phys. Res. A*, vol. A539, pp. 278–311, 2005.
- [11] A. S. Tremsin, O. H. W. Siegmund, J. V. Vallerga, J. S. Hull, and R. Abiad, "Cross strip readouts for photon counting detectors with high spatial and temporal resolution," *IEEE Trans. Nucl. Sci.*, vol. 51, no. 4, pp. 1707–1711, Aug. 2004.
- [12] D. S. Hussey, D. L. Jacobson, M. Arif, P. R. Huffman, R. E. Williams, and J. C. Cook, "New neutron imaging facility at the NIST," *Nucl. Instrum. Methods Phys. Res. A*, vol. A542, pp. 9–15, 2005.
- [13] V. F. Sears, "Neutron scattering lengths and cross sections," *Neutron News*, vol. 3, no. 3, pp. 26–37, 1992.